A Tractable and Accurate Cross-Layer Model for Multi-Hop MIMO Networks

Jia Liu Yi Shi Y. Thomas Hou
Bradley Department of Electrical and Computer Engineering
Virginia Polytechnic Institute and State University, Blacksburg, VA 24061

***Abstract*—MIMO-based communications have great potential to improve network capacity for multi-hop wireless networks. Although there has been significant progress on MIMO at the physical layer or single-hop communication, advances in the theory of MIMO for multi-hop wireless networks remain limited. This stagnation is mainly due to the lack of an accurate and more important, analytically tractable model that can be used by networking researchers. In this paper, we propose such a model to enable the networking community to carry out cross-layer research for multi-hop MIMO networks. In particular, at the physical layer, we develop a simple model for MIMO channel capacity computation that captures the essence of spatial multiplexing and transmit power limit without involving complex matrix operations and the water-filling algorithm. We show that the approximation gap in this model is negligible. At the link layer, we devise a space-time scheduling scheme called OBIC that significantly advances the existing zero-forcing beamforming (ZFBF) to handle interference in a multi-hop network setting. The proposed OBIC scheme employs simple algebraic computation on matrix dimensions to simplify ZFBF in a multi-hop network. As a result, we can characterize link layer scheduling behavior without entangling with beamforming details. Finally, we apply both the new physical and link layer models in cross-layer performance optimization for a multi-hop MIMO network.**

I. Introduction

Since its inception [1], [2], MIMO has been widely accepted as a key technology to increase wireless capacity. Researchers have shown that by employing multiple antennas on the transmitting and receiving nodes, wireless channel capacity can scale almost linearly with the number of antennas. Such capability is the driving force for the wide deployment of MIMO in wireless LAN (802.11n), WiMAX access networks (802.16), and 4G cellular networks (LTE).

Although there have been extensive studies on MIMO at the physical layer for point-to-point and cellular communications (see, e.g., [3] for an overview), fundamental understanding and results on MIMO in multi-hop networks remain limited, particularly from a cross-layer perspective. This stagnation is mainly due to the lack of an accurate and more importantly, tractable model that is amenable for analysis by networking researchers. Traditional signal processing and channel models for MIMO in communications research are clogged with complex matrix representations and operations, rendering enormous challenges for multi-hop network optimizations. Due to these challenges, most efforts on multi-hop MIMO networks to date [4]–[12] fall into the following two approaches.

The first approach is to formulate the problems by faithfully incorporating the MIMO channel and signal models without any loss of accuracy. However, the problem formulations under this approach soon become *intractable* due to the heavy burden from the underlying models. For example, Kim *et al.* studied a maxmin optimization problem in [4] for multi-hop MIMO backhaul networks where they formulated a nonlinear optimization problem to maximize the fair throughput of the access points in the network under the routing, MAC, and physical layer constraints. The physical layer in [4] is based on minimum mean square error (MMSE) beamforming. In [5], Chu and Wang also studied cross-layer algorithms for MIMO ad hoc networks where MMSE sequential interference cancellation technique (MMSE-SIC) was employed at the physical layer to maximize signal to interference and noise ratio (SINR). Due to the complex MMSE mechanics, the cross-layer optimization problems in [4] and [5] are intractable and the authors had to resort to heuristic algorithms.

The second approach is to simplify MIMO physical layer behavior so that tractable analysis can be developed for networking research. Although such approach is attractive, the problem with existing models under this approach suffer from "over simplification." That is, existing simple models ignore some important characteristics of MIMO and thus lead to results far from MIMO's achievable performance. In [6], [7], a simplified MIMO cross-layer model was employed to study different throughput optimization problems. By using this model, the network throughput performance can be characterized simply by counting the number of degrees of freedom (DoF) in the network. However, this model does not consider transmit power constraint and power allocation at each node in the network. Also, although some ideas of zero-forcing beamforming (ZFBF) were employed to handle interference, the proposed interference cancellation scheme at the link layer was not designed efficiently, resulting in a small DoF region and inferior throughput performance. Also, in [8]–[12], various studies on MAC designs and routing schemes are given based on very simple MIMO models that do not fully exploit MIMO physical capabilities.

The goal of this paper is to achieve the best of both approaches while avoiding their pitfalls. We want to construct a model for MIMO that is both *tractable* and *accurate* for cross-layer optimization. Our main contributions are as follows.

- At the physical layer, we devise a simple model for computing MIMO channel capacity. This model captures the essence of both spatial multiplexing and transmit power constraint. More importantly, this model does not

require complex matrices computation and complicated water-filling process (which does not admit a close-form solution). We show that the gap between our proposed model and the exact capacity model is negligible.

- At the link layer, we construct a model that takes into account the interference nulling/supression by exploiting ZFBF. More specifically, we propose a space-time scheduling scheme called OBIC (abbreviation of order-based interference cancelation). The proposed OBIC employs simple algebraic computation on matrix dimensions to model ZFBF in a multi-hop network. Moreover, by carefully arranging the cancellation order among the nodes, OBIC does not waste unnecessary DoF resources on interference mitigation, thus offering superior throughput performance than those in [6], [7].
- As an application, we use the proposed new models to study a cross-layer utility maximization problem for multi-hop MIMO networks. We show that the resulting optimization problem no longer involve complex matrix variables and operations. Further, the formulated problem shares a lot of similarities with those cross-layer optimization problems under single-antenna ad hoc networks, which have been actively studied in recent years. This suggests that new solutions to multi-hop MIMO networks may be developed by drawing upon the experiences gained for single-antenna ad hoc networks.

The remainder of this paper is organized as follows. Section II presents a new channel capacity model for MIMO at the physical layer. Section III presents a new link layer model called OBIC. In Section IV, as an application of our new models, we study a cross-layer optimization problem in a multi-hop MIMO network. Section V concludes this paper.

II. A Model for Physical Layer Capacity Computation

From networking research perspective, the most important aspect of physical layer modeling for MIMO is its channel capacity computation. In Section II-A, we first give background on MIMO channel capacity computation and analyze why it is difficult to work with for networking research. Then, in Section II-B, we propose a new model for MIMO channel capacity that is both simple and accurate.

A. Why Existing Physical Model for MIMO is Difficult to Use?

The channel of a MIMO link l is characterized by a matrix $\mathbf{H}_l$, as shown in Fig. 1. Communication over such a MIMO channel with n_t transmit antennas and n_r receive antennas can be described by

$$\mathbf{y}_l = \sqrt{\rho_l \alpha_l}\mathbf{H}_l\mathbf{x}_l + \mathbf{n}_l, \tag{1}$$

where $\mathbf{x}_l$, $\mathbf{y}_l$ and $\mathbf{n}_l$ denote the vectors of transmitted signal, received signal, and white Gaussian noise with unit variance, respectively. In (1), ρ_l represents the received SNR of the channel, $\alpha_l \in [0,1]$ represents the fraction of the transmit power that is assigned to link l (in the case when the source of link l also transmits on other links). As we shall see later in Section IV, α_l is useful to model the power allocation at each node if multi-hop multi-path routing is employed in the network. For the single link case in Fig. 1, we have $\alpha_l = 1$.

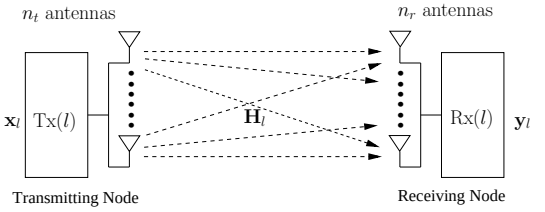

Fig. 1. A MIMO channel.

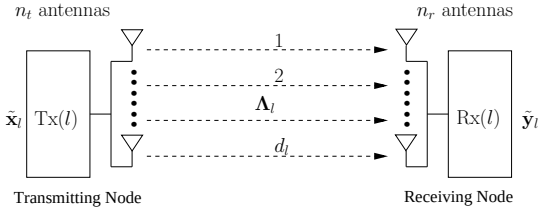

Fig. 2. The equivalent parallel scalar channels after transformation.

The channel gain matrix $\mathbf{H}_l$ is typically assumed to be a complex random matrix with each of its entries being i.i.d. Gaussian distributed [13] with zero mean and unit variance. From basic linear algebra, we know that by singular value decomposition (SVD), the channel model in (1) can be written as $\mathbf{y}_l = \sqrt{\rho_l\alpha_l}\mathbf{U}_l\mathbf{\Lambda}_l\mathbf{V}_l^\dagger\mathbf{x}_l + \mathbf{n}_l$, where $\mathbf{U}_l$ and $\mathbf{V}_l$ are unitary matrices, $\mathbf{\Lambda}_l$ is a diagonal matrix with the singular values of $\mathbf{H}_l$ on its main diagonal. By letting $\tilde{\mathbf{x}}_l = \mathbf{V}_l^\dagger\mathbf{x}_l$, $\tilde{\mathbf{y}}_l = \mathbf{U}_l^\dagger\mathbf{y}_l$, and $\tilde{\mathbf{n}}_l = \mathbf{U}_l^\dagger\mathbf{n}_l$, the channel model can be re-written as

$$\tilde{\mathbf{y}}_l = \sqrt{\rho_l\alpha_l}\mathbf{\Lambda}_l\tilde{\mathbf{x}}_l + \tilde{\mathbf{n}}_l, \tag{2}$$

which is equivalent to a set of parallel channels shown in Fig. 2. The number of non-zero singular values (i.e., non-zero diagonal entries in $\mathbf{\Lambda}_l$) is $d_l \le \min\{n_t, n_r\}$, i.e., the rank of $\mathbf{H}_l$. The rank of $\mathbf{H}_l$ is also called the *degrees of freedom* (DoF), which measures the number of independent signaling dimensions that are available in the channel.

The capacity for the set of parallel channels in (2) can be found by the water-filling power allocation algorithm [1]:

$$\begin{aligned} C_l^{(\mathrm{wf})} &= \max_{\mathbf{Q}_l} W\log_2\det(\mathbf{I} + \rho_l\alpha_l\mathbf{H}_l\mathbf{Q}_l\mathbf{H}_l^\dagger) \\ &= \sum_{i=1}^{d_l} W\left(\log_2(\rho_l\alpha_l\mu\lambda_i)\right)_+, \end{aligned}$$

where W represents the bandwidth of the channel; $\mathbf{Q}_l = \mathbb{E}\{\mathbf{x}_l\mathbf{x}_l^\dagger\}$ is the input covariance matrix representing the power allocation of signal $\mathbf{x}_l$; $\det(\cdot)$ represents matrix determinant; $\mathbf{I}$ represents an $n_r \times n_r$ identity matrix; $(\cdot)_+$ represents $\max(0,\cdot)$; λ_i denotes an eigenvalue of matrix $\mathbf{H}_l\mathbf{H}_l^\dagger$ (having the same number of non-zero singular values in $\mathbf{\Lambda}_l$ and equal to the square of the singular values of $\mathbf{H}_l$); and μ is the optimal water-level satisfying $\sum_{i=1}^{d_l}(\mu - (\rho_l\alpha_l\lambda_i)^{-1})_+ = 1$.

Further, since $\mathbf{H}_l$ is a random matrix, the ergodic capacity

of such a fading MIMO channel can be computed as [14]:

$$C_{l,\text{ergodic}}^{(\text{wf})} = \mathbb{E}_{\mathbf{H}_l}[C_l^{(\text{wf})}] = W \sum_{i=1}^{d_l} \mathbb{E}_{\lambda_i} \left[(\log_2(\rho_l \alpha_l \mu \lambda_i))_+ \right]$$
$$= W \sum_{i=1}^{d_l} \int (\log_2(\rho_l \alpha_l \mu \lambda_i))_+ f_{\lambda_i}(\lambda) d\lambda \ , \quad (3)$$

where $\mathbb{E}_{\lambda_i}[\cdot]$ represents the expectation taken over the distribution of λ_i and $f_{\lambda_i}(\cdot)$ denotes the distribution of λ_i. Although (3) is the exact formula for computing MIMO channel capacity, there are some issues that prevent (3) from being easily adopted in cross-layer optimization.

1) To determine the eigenvalues λ_i of $\mathbf{H}_l\mathbf{H}_l^\dagger$, one needs to solve the characteristic polynomial equation. However, it is known that there is no formula for roots of polynomials of degree 5 or greater. Even for a cubic or quartic polynomial equation (corresponding to 3×3 and 4×4 MIMO channels), the root formula is cumbersome to use and the equation is often solved approximately by numerical methods instead. Further, due to the complexity in computing λ_i, it is even harder to determine the distribution of $f_{\lambda_i}(\cdot)$ from $\mathbf{H}_l\mathbf{H}_l^\dagger$.

2) Even if we have solved λ_i's for a given $\mathbf{H}_l$, it remains to solve the optimal water-level μ for the optimal power allocation. However, due to the discontinuity property of the water-filling solution, there is no closed-form solution to determine μ. Instead, μ can only be evaluated numerically.

3) Since it is difficult to determine λ_i, $f_{\lambda_i}(\cdot)$, and μ, computing the integration in (3) becomes a challenging task. Instead of integrating $(\log_2(\rho_l \alpha_l \mu \lambda_i))_+ f_{\lambda_i}(\cdot)$, we can calculate a sample mean of $(\log_2(\rho_l \alpha_l \mu \lambda_i))_+$ as an approximation for the expectation. However, this calculation requires a large number of random samples of $\mathbf{H}_l$ (so as to obtain a good approximation).

Due to the above difficulties, Eq. (3) cannot be readily used to offer tractable analysis in cross-layer optimization.

B. A Simple and Accurate Model for MIMO Channel Capacity

To avoid the difficulties incurred in using (3), we propose a simple and yet non-trivial model to approximate the MIMO channel capacity computation as follows:

$$C_l^{(\text{sim})} = W \cdot d_l \cdot \log_2 \left(1 + \frac{\rho_l \alpha_l}{d_l} \right). \quad (4)$$

The construction of (4) is based on the following intuition. First, note that in (3), the capacity is determined by the averaging behavior of the eigenvalues of $\mathbf{H}_l\mathbf{H}_l^\dagger$. Although these eigenvalues are random, in practice they tend to be i.i.d. faded. As a result, when averaged over a large number of channel realizations, the mean channel gain for each parallel spatial channel (see Fig. 2) is roughly the same. Therefore, we approximate the random matrix $\mathbf{H}_l$ by a *deterministic* identity matrix (i.e., we replace $\mathbf{H}_l$ by $\mathbf{I}_{d_l}$), thus eliminating the expectation computation. With such a simplification, it is easy to verify that the optimal water-filling scheme degenerates into a trivial equal power allocation since all spatial channels have equal gain. It then follows that the channel capacity can be roughly approximated by (4). The main benefit of (4) is that we no longer need to explicitly compute the eigenvalues of $\mathbf{H}_l\mathbf{H}_l^\dagger$, the p.d.f. of λ_i, the optimal water level μ, and the expectation function. Note that when $d_l = 1$, (4) is reduced to Shannon formula for single-antenna case.

TABLE I
NORMALIZED GAP VERSUS THE NUMBER OF ANTENNAS.

Number of antennas	Normalized gap	
	SNR = 20 dB	SNR = 30 dB
2	0.96%	0.82%
3	2.23%	1.87%
4	2.89%	2.39%
5	3.21%	2.73%
6	3.46%	2.93%
7	3.46%	3.08%
8	3.70%	3.23%

We now formally examine the accuracy of (4). First, we quantify the gap between (3) and (4) for one channel realization. We have the following lemma and its proof is given in [15].

Lemma 1. *For a MIMO link with instantaneous channel gain $\mathbf{H}_l$ of rank d_l, $\Delta C_l \triangleq C_l^{(\text{wf})} - C_l^{(\text{sim})} \approx W \sum_{i=1}^{d_l} \log_2 \lambda_i$ under a high SNR regime.*

Based on Lemma 1, we show the gap between (3) and (4) is small by showing $\mathbb{E}_{\mathbf{H}_l}[\sum_{i=1}^{d_l} \log \lambda_i]$ is negligibly small. We state the result in the following theorem and give a proof in Appendix A.

Theorem 1. *Under a high SNR regime, for a MIMO link with Gaussian random channel matrix $\mathbf{H}_l$ of rank d_l, the approximation gap incurred by the simple model in (4) is close to zero.*

To offer some quantitative insights on this gap, in Table I, we show the normalized gap between (3) and (4) for a MIMO channel under $\rho_l = 20$ dB and $\rho_l = 30$ dB, respectively. We vary the number of antennas from 2 to 8 (range for practical MIMO systems). We can see that the gap between the approximation and the exact capacity is indeed negligibly small. For example, with 4 antennas under 30 dB, the gap is only 2.39%.

III. LINK LAYER MODELING FOR MULTI-HOP MIMO NETWORKS

At the link layer, MIMO opens up new opportunities in space domain to mitigate interference. In Section III-A, we first describe zero forcing beamforming (ZFBF), which is a powerful MIMO interference mitigation technique. We also discuss its benefits and challenges in multi-hop network setting. In Section III-B, we propose a space-time scheduling scheme called OBIC and in Section III-C, we construct its mathematical model.

A. Zero-Forcing Beamforming: Benefits and Challenges

In cellular MIMO systems, one of the most powerful interference mitigation technique is called ZFBF [16], [17]. ZFBF uses multi-antenna arrays to steer beams toward the intended

receiver to increase SNR, while forming nulls to unintended receivers to avoid interference. In MIMO cellular systems, however, ZFBF is usually performed at the transmitter side. In this paper, we generalize ZFBF to multi-hop networks by allowing beamforming to be performed on both transmitter and receiver sides.

To see how the generalized ZFBF can be used in multi-hop MIMO networks, consider a network having L links among which L_0 links are active. We denote $\bar{\mathcal{I}}_l$ the set of links that interfere with the reception of link l's intended receiver, $l = 1, 2, \ldots, L_0$. We denote $\mathbf{H}_{\mathrm{Tx}(m),\mathrm{Rx}(l)}$ the interference channel gain matrix from transmitting node of interference link m ($\mathrm{Tx}(m)$) to receiving node of link l ($\mathrm{Rx}(l)$).

To extract the transmitted signal through a MIMO channel, a transmit beamforming matrix and a receive beamforming matrix are employed on the channel. Thus, the received signal at link l can be written as

$$\mathbf{y}_l = \sqrt{\rho_l \alpha_l}\, \underbrace{\mathbf{R}^{\dagger}_{\mathrm{Rx}(l)} \mathbf{H}_l \mathbf{T}_{\mathrm{Tx}(l)} \mathbf{x}_l}_{\text{Desired signal part}} + \underbrace{\sum_{m \in \bar{\mathcal{I}}_l} \sqrt{\rho_{m,l} \alpha_m} \mathbf{R}^{\dagger}_{\mathrm{Rx}(l)} \mathbf{H}_{\mathrm{Tx}(m),\mathrm{Rx}(l)} \mathbf{T}_{\mathrm{Tx}(m)} \mathbf{x}_m}_{\text{Interference part}} + \mathbf{n}_l, \ \forall l,$$

where $\rho_{m,l}$ denotes the interference-to-noise ratio (INR) from node $\mathrm{Tx}(m)$ to node $\mathrm{Rx}(l)$.

By exploiting the multi-antenna array at each node, it is possible to cancel out all interferences by judiciously configuring $\mathbf{T}$'s and $\mathbf{R}$'s. Specifically, we can configure $\mathbf{T}$'s and $\mathbf{R}$'s in such a way that

$$\mathbf{R}^{\dagger}_{\mathrm{Rx}(l)} \mathbf{H}_{\mathrm{Tx}(m),\mathrm{Rx}(l)} \mathbf{T}_{\mathrm{Tx}(m)} = \mathbf{0}, \quad \forall l, m \in \bar{\mathcal{I}}_l. \tag{5}$$

Note that if there exist non-trivial solutions to (5) (i.e., $\mathbf{R}_{\mathrm{Rx}(l)} \neq \mathbf{0}$, $\mathbf{T}_{\mathrm{Tx}(m)} \neq \mathbf{0}$, $\forall l, m \in \bar{\mathcal{I}}_l$), then it means that all L_0 links can be active simultaneously in an *interference-free* environment. Moreover, the ranks of $\mathbf{T}_{\mathrm{Tx}(l)}$ and $\mathbf{R}_{\mathrm{Rx}(l)}$ determine the maximum number of data streams z_l that can be transmitted over link l, i.e., $z_l \leq \min\{\mathrm{rank}(\mathbf{T}_{\mathrm{Tx}(l)}), \mathrm{rank}(\mathbf{R}_{\mathrm{Rx}(l)})\}$.

Although ZFBF's benefits are appealing, there remain significant challenges to employ it in multi-hop networks. This is because finding an optimal set of $\mathbf{T}$'s and $\mathbf{R}$'s satisfying (5) requires solving a large number of *bilinear* equations. Unlike linear equation systems, a general solution to bilinear equation systems remains unknown [18]. Thus, it becomes an intractable problem to design scheduling schemes based on solving (5).

B. OBIC: Basic Idea

We find that the specific element configurations in $\mathbf{T}$'s and $\mathbf{R}$'s are more closely tied to beamforming design than to link layer scheduling. Therefore, instead of focusing on solving (5), we propose to reposition ourselves to exploit matrix dimension constraints that are sufficient for (5) to hold. By doing so, we can characterize the link layer scheduling performance without entangling with the details of beamforming designs.

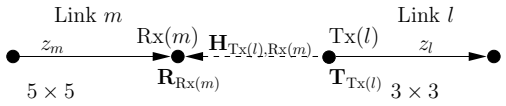

Fig. 3. A two-link example.

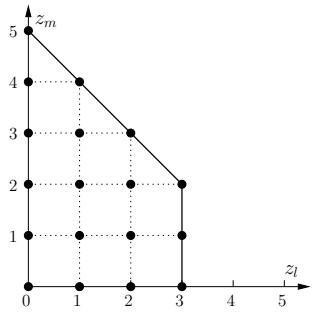

Fig. 4. DoF region of two-link example.

To understand how we can extract the matrix dimension constraints for ZFBF-based scheduling, we first use a simple two-link network shown in Fig. 3 as an example. In this network, link l has 3 antennas on each side and link m has 5 antennas on each side. For this simple network, we can first choose a $\mathbf{T}_{\mathrm{Tx}(l)}$ arbitrarily without considering link m's existence. Suppose that $\mathbf{T}_{\mathrm{Tx}(l)}$ is full-rank (i.e., 3 data streams being transmitted). Next, we choose an $\mathbf{R}_{\mathrm{Rx}(m)}$ to cancel the interference from link l, while receiving data streams from its desired transmitter. This is equivalent to solving $(\mathbf{H}_{\mathrm{Tx}(l),\mathrm{Rx}(m)} \mathbf{T}_{\mathrm{Tx}(l)})^{\dagger} \mathbf{R}_{\mathrm{Rx}(m)} = \mathbf{0}$ with $\mathbf{T}_{\mathrm{Tx}(l)}$ already determined. This implies that all column vectors in $\mathbf{R}_{\mathrm{Rx}(m)}$ have to lie in the null space of $(\mathbf{H}_{\mathrm{Tx}(l),\mathrm{Rx}(m)} \mathbf{T}_{\mathrm{Tx}(l)})^{\dagger}$. The dimension of the null space in this case is $\dim(\mathrm{null}((\mathbf{H}_{\mathrm{Tx}(l),\mathrm{Rx}(m)} \mathbf{T}_{\mathrm{Tx}(l)})^{\dagger})) = 5 - 3 = 2$, meaning that $\mathrm{Rx}(m)$ can receive up to 2 streams. Note that links l and m are both active in an *interference-free* environment. Further, by varying the ranks of $\mathbf{T}_{\mathrm{Tx}(l)}$ and $\mathbf{R}_{\mathrm{Rx}(m)}$, it is easy to verify that the achievable DoF region under this ZFBF-based scheme is the trapezoid shown in Fig. 4.[1] Observe that the scheduling scheme in this two-link example is performed in an *ordered* fashion: we arbitrarily choose a $\mathbf{T}_{\mathrm{Tx}(l)}$ first, and then choose an $\mathbf{R}_{\mathrm{Rx}(m)}$ such that the interference can be eliminated.

We now extend this order-based interference cancellation idea to a three-link example shown in Fig. 5, which is more complicated than the previous example. Here, each receiving node of a link is being interfered by the transmitting nodes of other links. For this example, we can start with a scheduling order for the six nodes. Such a scheduling order will be subject to an optimization in Section III-C. Suppose the scheduling order for the six nodes is $\mathrm{Tx}(l) \rightarrow \mathrm{Rx}(m) \rightarrow \mathrm{Rx}(l) \rightarrow \mathrm{Tx}(m) \rightarrow \mathrm{Tx}(n) \rightarrow \mathrm{Rx}(n)$. Then, through the following scheduling decision, we can show that the stream combination $(1, 1, 2)$ is achievable.

[1]Note that the achievable DoF region in Fig. 4 coincides with the maximum DoF region described in [19, Theorem 2]. Thus, for this two-link example, the proposed scheduling scheme is an optimal scheduling scheme.

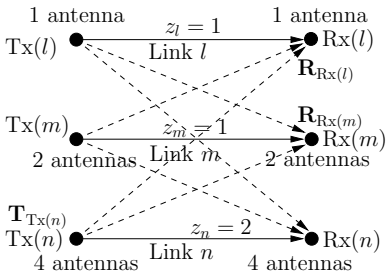

Fig. 5. A three-link example.

1) $\mathrm{Tx}(l)$: Since nodes $\mathrm{Tx}(l)$ is the first to be scheduled, it does not have any interference to concern about. Also, since $\mathrm{Tx}(l)$ has only 1 antenna, we can let $\mathrm{Tx}(l)$ transmit 1 data stream;

2) $\mathrm{Rx}(m)$: Since $\mathrm{Rx}(m)$ is scheduled after $\mathrm{Tx}(l)$, it needs to suppress the interference from $\mathrm{Tx}(l)$, i.e., solving $(\mathbf{H}_{\mathrm{Tx}(l),\mathrm{Rx}(m)}\mathbf{T}_{\mathrm{Tx}(l)})^{\dagger}\mathbf{R}_{\mathrm{Rx}(m)} = \mathbf{0}$. We have $\dim(\mathrm{null}((\mathbf{H}_{\mathrm{Tx}(l),\mathrm{Rx}(m)}\mathbf{T}_{\mathrm{Tx}(l)})^{\dagger})) = 2-1 = 1$, i.e., we can let $\mathrm{Rx}(m)$ receive 1 stream in this case;

3) $\mathrm{Rx}(l)$: Since no interfering transmitting node is scheduled before $\mathrm{Rx}(l)$, $\mathrm{Rx}(l)$ does not need to concern about any interference. Given $\mathrm{Rx}(l)$ has only 1 antenna, we can let it receive 1 stream;

4) $\mathrm{Tx}(m)$: Following the similar argument as for $\mathrm{Rx}(m)$, we can let $\mathrm{Tx}(m)$ transmit 1 stream;

5) $\mathrm{Tx}(n)$: Since $\mathrm{Tx}(n)$'s transmission should not interfere with $\mathrm{Rx}(l)$ and $\mathrm{Rx}(m)$, it follows that $\mathbf{T}_{\mathrm{Tx}(n)}$ should satisfy $\begin{bmatrix} \mathbf{R}^{\dagger}_{\mathrm{Rx}(l)}\mathbf{H}_{\mathrm{Tx}(n),\mathrm{Rx}(l)} \\ \mathbf{R}^{\dagger}_{\mathrm{Rx}(m)}\mathbf{H}_{\mathrm{Tx}(n),\mathrm{Rx}(m)} \end{bmatrix}\mathbf{T}_{\mathrm{Tx}(n)} = \mathbf{0}$. Since $\dim\left(\mathrm{null}\begin{bmatrix} \mathbf{R}^{\dagger}_{\mathrm{Rx}(l)}\mathbf{H}_{\mathrm{Tx}(n),\mathrm{Rx}(l)} \\ \mathbf{R}^{\dagger}_{\mathrm{Rx}(m)}\mathbf{H}_{\mathrm{Tx}(n),\mathrm{Rx}(m)} \end{bmatrix}\right) = 4-(1+1) = 2$, we can schedule 2 data streams at $\mathrm{Tx}(n)$;

6) $\mathrm{Rx}(n)$: Following a similar analysis as in 5), it can be shown that 2 streams can be scheduled at $\mathrm{Rx}(n)$.

The idea in the three-link example can be synthesized for a general multiple-link setting. The essence of this scheduling scheme is to perform interference cancellation successively based on an ordered node list:

- If a node is transmitting, then it is only necessary to ensure that its transmissions do not interfere with previously scheduled receiving nodes in the ordered node list. It does not need to expend precious DoF resources to null its interference to those receiving nodes to be scheduled after itself in the node list.
- If a node is receiving, it only needs to suppress interference from transmitting nodes scheduled before itself in the node list. It does not need to concern interfering transmitting nodes to be scheduled after itself.

The interference cancellation behavior described above offers the basic idea for a node-based scheduling scheme. For easy reference, we call this scheduling scheme OBIC (order-based interference cancelation). Additional quantitative constraints on DoF on each transmitting and receiving node (as shown in last two examples) will be discussed in the next section. Fig. 6 shows the flow chart of the OBIC scheme.

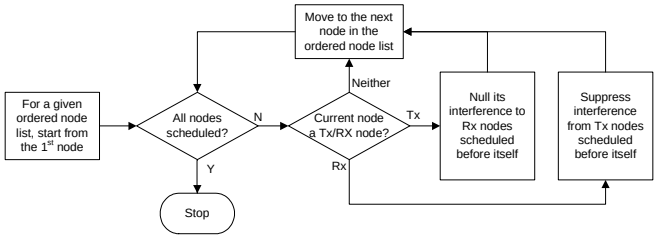

Fig. 6. The flow chart of OBIC scheduling scheme.

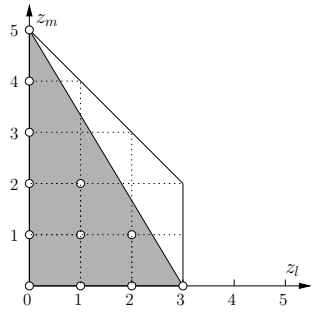

Fig. 7. Achievable DoF region comparison between OBIC and CiM for the example in Fig. 3.

Remark 1. In [6], Hamdaoui and Shin proposed several interference avoidance schemes based on ZFBF. For the so-called CiM scheme (the best among the proposed schemes in [6]), the authors also recognized that interference can be cancelled by either the transmitting or the receiving node of an interference link. However, without employing a node-based sequential scheduling, it is impossible to know which node should perform interference mitigation. As a result, the CiM scheme requires both the transmitting and receiving nodes of an interference link to expend precious DoFs for interference cancellation (c.f. [6, Eq. (10)]). This approach adversely leads to a much smaller DoF region. As an example, we compare the performance of OBIC and the CiM model on the simple two-link example in Fig. 3. Under the CiM model, it is not difficult to verify that the achievable DoF region is the shaded triangle in Fig. 7, representing the convex hull of the white dots, which are the DoF combinations directly achievable under CiM. It can be seen that this region is smaller than the achievable DoF region by OBIC. In general, it can be shown that the DoF region achieved under the CiM model is always a subset of that under the OBIC [15].

Remark 2. We point out that for the three-link network example in Fig. 5, a larger DoF region can be achieved by interference alignment (IA) [20]. The basic idea of IA is that by aligning the interference from two interfering transmitters at each receiving node, the interference from different nodes becomes dependent, implying a smaller rank of the effective interference channel. This in turn leads to a higher dimensional null space that can be exploited for data transmissions. We note, however, that IA also has its limitations. IA was proposed for the classical interference channel in the context of network information theory [21], where the channel possesses

a "fully-connected" structure. That is, each link in the network is interfered by all remaining links. For general multi-hop network topology where the full connectivity may not hold, the achievable DoF region of IA remains an open problem.

C. OBIC: A Mathematical Model

Having introduced the basic idea of OBIC, we now develop its mathematical model. We represent the topology of a multi-hop MIMO network by a directed graph, denoted by $\mathcal{G} = \{\mathcal{N}, \mathcal{L}\}$, where $\mathcal{N}$ and $\mathcal{L}$ are the sets of nodes and all possible MIMO links, respectively. Suppose that the cardinalities of the sets $\mathcal{N}$ and $\mathcal{L}$ are $|\mathcal{N}| = N$ and $|\mathcal{L}| = L$, respectively. In this paper, we assume that scheduling operates in a frame-by-frame system with T time slots in each frame. We remark that this time-slotted assumption is not a necessary restriction. For this work, there is no fundamental distinction between time and frequency dimensions. Thus, the time slot index t in the mathematical modeling described below could equivalently be used to describe frequency slots or even a time-frequency tuple.

Modeling an Ordered Node List. Refer to Fig. 6 and the discussion in Section III-B. Before we start scheduling on a node, we must have an ordered node list, which will be subject to an optimization.

To model an ordered node list that can be optimized, we define the following binary variable. For $i, j \in \mathcal{N}$, $i \neq j$, we let $\pi_{ij}(t) = 1$ if node j is scheduled after node i in time slot t and 0 otherwise. It is easy to see that $\pi_{ij}(t)$ must satisfy the following two properties.

i) *Mutual exclusiveness*: If node j is scheduled after node i (i.e., $\pi_{ij}(t) = 1$), then it also implies that node i is before node j (i.e., $\pi_{ji}(t) = 0$). This relationship can be modeled as

$$\pi_{ij}(t) + \pi_{ji}(t) = 1, \quad \forall i, j \in \mathcal{N} : i \neq j, \ \forall t. \tag{6}$$

ii) *Transitivity*: If node j is scheduled after i (i.e., $\pi_{ij} = 1$) and node k is scheduled after node j (i.e., $\pi_{jk} = 1$), then it implies that node k is scheduled after node i (i.e., $\pi_{ik} = 1$). To model this transitivity property, we have the following lemma and refer readers to [15] for the details of the proof due to space limitation.

Lemma 2. *Let $\Omega(\cdot)$ be a one-on-one mapping from each element in the set $\mathcal{N}$ to a natural number in $\{1, 2, \ldots, N\}$. For nodes $i, j, k \in \mathcal{N}$ with $\Omega(i) < \Omega(j) < \Omega(k)$, the following two constraints are sufficient to describe the transitivity relationship among nodes node triplet i, j, and k:*

$$1 \leq \pi_{ij}(t) + \pi_{jk}(t) + \pi_{ki}(t) \leq 2. \tag{7}$$

The constraint in (7) can be interpreted in a logical sense. It is easy to see that $1 \leq \pi_{ij}(t) + \pi_{jk}(t) + \pi_{ki}(t) \leq 2$ implies that at least 1 and at most 2 π-variables can be equal to one. If not, then we have either $\pi_{ij}(t) = \pi_{jk}(t) = \pi_{ki}(t) = 0$ or $\pi_{ij}(t) = \pi_{jk}(t) = \pi_{ki}(t) = 1$, both of which cannot be true since the ordering for i, j, and k would then form a loop.

Modeling the Transmitting Node Behavior. Next, we model the block in Fig. 6 where a node i is scheduled to be a transmitting node. Note that in each time slot t, $1 \leq t \leq T$, due to half-duplex, each node either transmit, receive, or be idle. To model half-duplex, we introduce two groups of binary variables $g_i(t)$'s and $h_i(t)$'s as follows. $g_i(t) = 1$ if node i is transmitting in time slot t and 0 otherwise; $h_i(t) = 1$ if node i is receiving in time slot t and 0 otherwise. Then, the half-duplex constraint can be characterized by

$$g_i(t) + h_i(t) \leq 1, \quad \forall i, t. \tag{8}$$

We assume that scattering is rich enough in the environment such that all channel matrices are of full-rank. As a result, the number of data streams that a node can transmit or receive is limited by its number of antennas and we have the following two constraints:

$$g_i(t) \leq \sum_{l \in \mathcal{L}_i^{\mathrm{Out}}} z_l(t) \leq g_i(t) A_i, \tag{9}$$

$$h_i(t) \leq \sum_{l \in \mathcal{L}_i^{\mathrm{In}}} z_l(t) \leq h_i(t) A_i, \tag{10}$$

where $\mathcal{L}_i^{\mathrm{Out}}$ and $\mathcal{L}_i^{\mathrm{In}}$ represent the sets of outgoing and incoming links at node i, respectively; $z_l(t)$ denotes the number of data streams over link l in time slot t, and A_i represents the number of antennas at node i.

From Fig. 6, we see that the data streams transmitted by node i should not interfere with those receiving nodes scheduled previously. This is equivalent to saying that the transmission beamforming vectors in $\mathbf{T}_i$ should lie in the null space of the stacked matrix formed by stacking all $\mathbf{R}_j^{\dagger}\mathbf{H}_{i,j}$ matrices, where j denotes a previously scheduled receiving node that could be interfered by node i. That is,

$$\mathbf{T}_i \in \mathrm{null}\left[\begin{array}{c} \vdots \\ \mathbf{R}_j^{\dagger}\mathbf{H}_{i,j} \\ \vdots \end{array}\right], \begin{array}{l} j \in \mathcal{I}_i \text{ and } j \text{ is} \\ \text{scheduled before } i \\ \text{(i.e., } \pi_{ji} = 1\text{),} \end{array} \tag{11}$$

where $\mathcal{I}_i$ represents the set of nodes within the interference range of node i. For convenience, we let $\mathbf{S}$ denote the stacked matrix in (11). Note that $\sum_{l \in \mathcal{L}_i^{\mathrm{Out}}} z_l(t)$ is the number of data streams that node i transmits in time slot t. Thus, from (11), we have that $\sum_{l \in \mathcal{L}_i^{\mathrm{Out}}} z_l(t)$ should be less than or equal to the nullity of $\mathbf{S}$, i.e., $\sum_{l \in \mathcal{L}_i^{\mathrm{Out}}} z_l(t) \leq \mathrm{null}(\mathbf{S})$. Also, note that the rank of $\mathbf{S}$ is $\sum_{j \in \mathcal{I}_i} \pi_{ji}(t) \sum_{l:\mathrm{Rx}(l)=j}^{\mathrm{Tx}(l)\neq i} z_l(t)$. Therefore, according to rank-nullity theorem [22] (i.e., $\mathrm{rank}(\mathbf{S}) + \mathrm{null}(\mathbf{S})$ is equal to the number of columns in $\mathbf{S}$), we can model the dimensional constraint as follows: for all $i, j \in \mathcal{N}$ and for all $t \in [1, \ldots, T]$,

$$\sum_{l \in \mathcal{L}_i^{\mathrm{Out}}} z_l(t) + \sum_{j \in \mathcal{I}_i} \pi_{ji}(t) \sum_{\substack{l:\mathrm{Rx}(l)=j \\ \mathrm{Tx}(l)\neq i}} z_l(t) \leq A_i + (1 - g_i(t))M. \tag{12}$$

In (12), M is a sufficiently large number (e.g., we can set $M = \sum_{j \in \mathcal{I}_i} A_i$). When node i is a transmission node (i.e., $g_i(t) = 1$), then (12) is reduced to the rank-nullity condition with respect to $\mathbf{S}$. Otherwise, if node i is scheduled to be a

receiving node or in idle status (i.e., $g_i(t) = 0$), then (12) trivially holds due to the large value of M.

We note that the nonlinear terms $\pi_{ji}(t)\sum_{l:\mathrm{Rx}(l)=j}^{\mathrm{Tx}(l)\neq i} z_l(t)$ in (12) could complicate optimizations. To remove these nonlinear terms, we can introduce a new integer variable $\phi_{ji}(t)$ and reformulate (12) as follows:

$$\sum_{l\in\mathcal{L}_i^{\mathrm{Out}}} z_l(t) + \sum_{j\in\mathcal{I}_i} \phi_{ji}(t) \le A_i + (1-g_i(t))M, \qquad (13)$$

where $\phi_{ji}(t)$, $\forall i \in \mathcal{N}$, $j \in \mathcal{I}_i$, $\forall t \in [1,\ldots,T]$, satisfies the following constraints:

$$\phi_{ji}(t) \le \textstyle\sum_{l:\mathrm{Rx}(l)=j}^{\mathrm{Tx}(l)\neq i} z_l(t), \qquad (14)$$

$$\phi_{ji}(t) \le A_i\pi_{ji}(t), \qquad (15)$$

$$\phi_{ji}(t) \ge A_i\pi_{ji}(t) - A_i + \textstyle\sum_{l:\mathrm{Rx}(l)=j}^{\mathrm{Tx}(l)\neq i} z_l(t). \qquad (16)$$

It is easy to verify that this set of new constraints (13)–(16) is equivalent to (12).

Modeling the Receiving Node Behavior. Similarly, for the block in Fig. 6 where a node i is scheduled to be a receiving node, we can derive the following constraints: for all $i, j \in \mathcal{N}$ and for all $t \in [1,\ldots,T]$,

$$\textstyle\sum_{l\in\mathcal{L}_i^{\mathrm{In}}} z_l(t) + \sum_{j\in\mathcal{I}_i} \varphi_{ji}(t) \le A_i + (1-h_i(t))M, \qquad (17)$$

$$\varphi_{ji}(t) \le \textstyle\sum_{l:\mathrm{Tx}(l)=j}^{\mathrm{Rx}(l)\neq i} z_l(t), \qquad (18)$$

$$\varphi_{ji}(t) \le A_i\pi_{ji}(t), \qquad (19)$$

$$\varphi_{ji}(t) \ge A_i\pi_{ji}(t) - A_i + \textstyle\sum_{l:\mathrm{Tx}(l)=j}^{\mathrm{Rx}(l)\neq i} z_l(t). \qquad (20)$$

Link Capacity Computation under OBIC. In Section II, we proposed a simple and accurate physical layer model to approximate the capacity of a single MIMO link. We are now ready to further extend (4) to approximate the capacity of each MIMO link under OBIC. First, we note that there is no interference among links due to ZFBF. Thus, as the single link case in Section II, the capacity of each link under OBIC is not affected by interference. However, compared with the single MIMO link case, a key difference in OBIC is that each active link l now transmits z_l data streams instead of d_l and $z_l \le d_l$. In this case, one may conjecture that a simple way to modify (4) for OBIC is to replace d_l with z_l. Indeed, the following theorem says that such an extension is correct and its rigorous proof is provided in [15].

Theorem 2. *Under OBIC, each MIMO link's capacity in time slot t can be approximated as*

$$C_l(t) = W \cdot z_l(t) \cdot \log_2\left(1 + \frac{\rho_l\alpha_l(t)}{z_l(t)}\right). \qquad (21)$$

Moreover, under a high SNR regime, the approximation gap incurred by (21) is negligible.

IV. Application in Multi-Hop Networks

In Sections II and III, we have developed two models for the physical layer and the link layer in multi-hop networks, respectively. In this section, we will show how to apply them for cross-layer optimization in multi-hop MIMO networks. We consider a generic utility maximization problem involving a set of sessions, $\mathcal{F}$, in an ad hoc network. Denote $\mathrm{src}(f)$ and $\mathrm{dst}(f)$ the source and destination nodes of session $f \in \mathcal{F}$, respectively. Denote $r(f)$ the flow rate of session f and $r_l(f)$ the flow rate on link l that is attributed to session $f \in \mathcal{F}$, respectively. Denote $C_l(t)$ the capacity of link l in time-slot t. For stability, we have the following constraints on the flow rates:

$$\textstyle\sum_{f\in\mathcal{F}} r_l(f) \le \frac{1}{T}\sum_{t=1}^{T} C_l(t), \quad \forall l. \qquad (22)$$

At the network layer, different routing schemes can be adopted. Under any routing scheme, the flow balance constraints must hold at each node $i \in \mathcal{N}$.

$$\textstyle\sum_{l\in\mathcal{L}_i^{\mathrm{Out}}} r_l(f) - \sum_{l\in\mathcal{L}_i^{\mathrm{In}}} r_l(f) = r(f), \text{ if } i = \mathrm{src}(f), \quad (23)$$

$$\textstyle\sum_{l\in\mathcal{L}_i^{\mathrm{Out}}} r_l(f) = \sum_{l\in\mathcal{L}_i^{\mathrm{In}}} r_l(f), \text{ if } i \neq \mathrm{src}(f), \mathrm{dst}(f), \quad (24)$$

$$\textstyle\sum_{l\in\mathcal{L}_i^{\mathrm{In}}} r_l(f) - \sum_{l\in\mathcal{L}_i^{\mathrm{Out}}} r_l(f) = r(f), \text{ if } i = \mathrm{dst}(f). \quad (25)$$

It can be easily verified that if (23) and (24) are satisfied, then (25) is automatically satisfied. As a result, it is not necessary to list (25) in problem formulation once we have both (23) and (24).

When a node is transmitting simultaneously on more than one outgoing link, it is necessary to consider power allocation among $\mathcal{L}_i^{\mathrm{Out}}$ at node i. Recall that $\alpha_l(t) \in [0,1]$ represent a fraction of transmit power allocated to link l in time-slot t. Then, for each node i in time-slot t, we have

$$\textstyle\sum_{l\in\mathcal{L}_i^{\mathrm{Out}}} \alpha_l(t) \le g_n(t), \quad \forall n, t. \qquad (26)$$

The constraint in (26) ensures that the sum of transmit power of all outgoing links at node i does not exceed the power limit. In the case when node i is not in transmission mode, then $g_i(t) = 0$ and $\alpha_l(t) = 0$ for all $l \in \mathcal{L}_i^{\mathrm{Out}}$.

Consider a utility function for each session, $u\big(r(f)\big)$, which we assume is concave. Then a general MIMO network utility maximization (MIMO-NUM) problem can be formulated as follows.

MIMO-NUM

max $\sum_{f=1}^{F} u\big(r(f)\big)$

s.t. Network layer flow-balance routing constraints in (23) and (24);
Link capacity constraints in (22);
OBIC based link layer constraints in (6), (7), (8), (9), (10) and (13)–(20);
Simplified MIMO physical layer model in (21) and (26).

Two remarks are in order. 1) *Tractability.* Recall that existing MIMO cross-layer optimization involves many matrix variables in the capacity calculation and ZFBF scheduling, making network level research quite challenging. With our simple models, matrix variables no longer appear in the MIMO-NUM problem, which significantly simplifies formulation and reduces computational complexity. 2) *Solvability.* By using our simple models, the MIMO-NUM problem is reduced to a similar mathematical form as a NUM problem for single-antenna ad hoc networks. Note that although the OBIC part

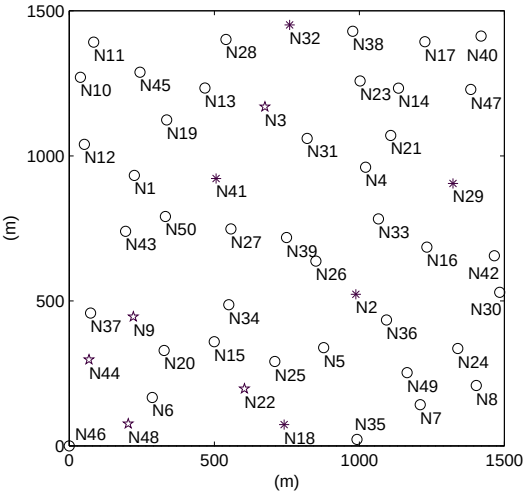

Fig. 8. A 50-node 5-session multi-hop MIMO network.

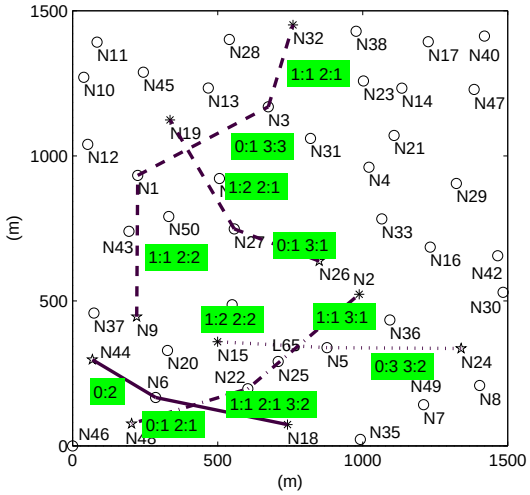

Fig. 9. Scheduling result on each link.

is unique, it is of linear form and can be handled easily. This suggests that we can take advantage of the existing experiences gained from single-antenna ad hoc networks in the literature to develop solutions.

As an example to illustrate the solvability of our MIMO-NUM formulation, we consider a multi-hop MIMO network consisting of 50 nodes that are uniformly distributed in a square region of 1500m $\times$ 1500m (see Fig. 8). Each node in the network is equipped with 4 antennas and the maximum power for each node is 100 mW. The channel bandwidth is 20 MHz. The path-loss index is 3.5. There are 5 sessions in the network: N26 to N19, N44 to N18, N24 to N15, N48 to N2, and N9 to N32, respectively. Suppose that minimum-hop routing is employed at the network layer. The objective is to maximize the sum of the end-to-end session rates, i.e., $u\big(r(f)\big) = r(f)$. Suppose that there are 4 time slots in each time frame, i.e., $T = 4$. Given these parameters and network settings, the MIMO-NUM problem is now completely specified. We can use CPLEX solver to obtain an optimal solution.

The optimal scheduling ordering for each node in each time slot is listed in Table II. In this table, each column gives the node ordering for scheduling in a given time slot of a frame. For example, in the first time slot, the optimal ordering of the nodes is $N19 \rightarrow N18 \rightarrow \ldots \rightarrow N2$.

Fig. 9 shows the routing paths for each session and optimal scheduling solution (shown in shaded boxes). As an example, the shaded box next to the link from N6 to N18 contains "1:1 2:1 3:2," which means that in time slots 1, 2, 3, there are 1, 1, and 2 streams on this link, respectively. In time slot 4, the link is not transmitting. Based on the number of streams, the simple physical layer model (21) and the link capacity constraint in (22), the optimal session rates (in Mb/s) are: 60.4 for N26 $\rightarrow$ N19, 151 for N44 $\rightarrow$ N18, 102 for N24 $\rightarrow$ N15, 36.6 for N48 $\rightarrow$ N2, and 57.2 for N9 $\rightarrow$ N32.

TABLE II
OPTIMAL NODE ORDERING IN EACH TIME SLOT OF A FRAME.

	Time Slot 1	Time Slot 2	Time Slot 3	Time Slot 4
1st	N19	N48	N24	N24
2nd	N18	N27	N22	N32
3rd	N44	N32	N44	N26
4th	N15	N15	N9	N48
5th	N26	N9	N15	N18
6th	N22	N19	N27	N24
7th	N5	N44	N32	N9
8th	N48	N26	N26	N22
9th	N6	N18	N19	N5
10th	N27	N2	N18	N6
11th	N24	N24	N6	N15
12th	N32	N22	N5	N19
13th	N3	N5	N48	N2
14th	N1	N3	N1	N27
15th	N9	N1	N3	N1
16th	N2	N6	N2	N3

V. CONCLUSION

Existing models for MIMO suffer from either intractability or inaccuracy when they are employed to study multi-hop MIMO networks. We proposed a tractable and accurate model for MIMO that is amenable for cross-layer analysis in multi-hop setting. Our contributions included a model at the physical layer and a model at the link layer. At the physical layer, we proposed a simple model to compute MIMO channel capacity that captures the essence of spatial multiplexing and transmit power limit without involving complex matrix operations and the water-filling algorithm. We proved that the approximation gap in this physical layer model is negligible. At the link layer, we proposed a scheduling scheme called OBIC that is based on ZFBF interference mitigation. The proposed OBIC scheme cuts through the complexity associated with beamforming designs in a multi-hop network by using simple algebraic computation. This allows us to explore the link layer scheduling performance without entangling with beamforming details. By applying the proposed cross-layer model to a general NUM problem, we validate its efficacy in practice. The results in this paper offer an important analytical tool to fully exploit

the potential of MIMO in multi-hop networks.

ACKNOWLEDGEMENT

The work of Y.T. Hou, J. Liu, and Y. Shi was supported in part by the National Science Foundation (NSF) under Grant CNS-0721421 and Office of Naval Research (ONR) under Grant N00014-08-1-0084.

REFERENCES

[1] I. E. Telatar, "Capacity of multi-antenna Gaussian channels," *European Trans. Telecomm.*, vol. 10, no. 6, pp. 585–596, Nov. 1999.

[2] G. J. Foschini, "Layered space-time architecture for wireless communication in a fading envorinment when using multi-element antennas," *Bell Labs Tech. J.*, vol. 1, no. 2, pp. 41–59, 1996.

[3] E. Biglieri, R. Calderbank, A. Constantinides, A. Goldsmith, A. Paulraj, and H. V. Poor, *MIMO Wireless Communications*. Cambridge University Press, Jan. 2007.

[4] S.-J. Kim, X. Wang, and M. Madihian, "Cross-layer design of wireless multihop backhaul networks with multiantenna beamforming," *IEEE Trans. Mobile Comput.*, vol. 6, no. 11, pp. 1259–1269, Nov. 2007.

[5] S. Chu and X. Wang, "Opportunistic and cooperative spatial multiplexing in MIMO ad hoc networks," in *Proc. ACM Mobihoc*, Hong Kong SAR, China, May 26-30, 2008, pp. 63–72.

[6] B. Hamdaoui and K. G. Shin, "Characterization and analysis of multihop wireless MIMO network throughput," in *Proc. ACM Mobihoc*, Montréal, Québec, Canada, Sep. 2007, pp. 120–129.

[7] R. Bhatia and L. Li, "Throughput optimization of wireless mesh networks with MIMO links," in *Proc. IEEE INFOCOM*, Anchorage, AK, May 6-12, 2007, pp. 2326–2330.

[8] M. Hu and J. Zhang, "MIMO ad hoc networks: Medium access control, saturation throughput, and optimal hop distance," *Special Issue on Mobile Ad Hoc Networks, Journal of Communications and Networks*, pp. 317–330, Dec. 2004.

[9] K. Sundaresan and R. Sivakumar, "Routing in ad hoc networks with MIMO links," in *Proc. IEEE International Conf. on Network Protocols*, Boston, MA, U.S.A., Nov. 2005, pp. 85–98.

[10] S. Y. Oh, M. Gerla, and J.-S. Park, "MIMO and TCP: A case for cross-layer design," in *Proc. IEEE MILCOM*, Orlando, FL, Oct. 29-31, 2007.

[11] S. Y. Oh, M. Gerla, P. Zhao, B. Daneshrad, G. Pei, and J. H. Kim, "MIMO-CAST: A cross-layer ad hoc multicast protocol using MIMO radios," in *Proc. IEEE MILCOM*, Orlando, FL, Oct. 29-31, 2007.

[12] J.-S. Park, A. Nandan, M. Gerla, and H. Lee, "SPACE-MAC: Enabling spatial reuse using MIMO channel-aware MAC," in *Proc. IEEE ICC*, Seoul, Korea, May 16-20, 2005, pp. 3642–3646.

[13] A. M. Tulino and S. Verdú, *Random Matrix Theory and Wireless Communications*. Hanover, MA: now Publishers Inc., 2004.

[14] A. Goldsmith, S. A. Jafar, N. Jindal, and S. Vishwanath, "Capacity limits of MIMO channels," *IEEE J. Sel. Areas Commun.*, vol. 21, no. 1, pp. 684–702, Jun. 2003.

[15] J. Liu, Y. Shi, and Y. T. Hou, "A tractable and accurate cross-layer model for multi-hop MIMO ad hoc networks," *Technical Report, Department of ECE, Virginia Tech*, Jul. 2009. [Online]. Available: http://filebox.vt.edu/users/kevinlau/publications

[16] L.-U. Choi and R. D. Murch, "A transmit preprocessing technique for multiuser MIMO systems using a decomposition approach," *IEEE Trans. Wireless Commun.*, vol. 3, no. 1, pp. 20–24, Jan. 2004.

[17] Q. H. Spencer, A. L. Swindlehurst, and M. Haardt, "Zero-forcing methods for downlink spatial multiplexing in multiuser MIMO channels," *IEEE Trans. Signal Process.*, vol. 52, no. 2, pp. 461–471, Feb. 2004.

[18] S. Roman, *Advanced Linear Algebra*. New York, NY: Springer, 2007.

[19] S. A. Jafar and M. J. Fakhereddin, "Degrees of freedom for the MIMO interference channel," *IEEE Trans. Inf. Theory*, vol. 53, no. 7, pp. 2637–2642, Jul. 2007.

[20] V. R. Cadambe and S. A. Jafar, "Interference alignment and degrees of freedom of the K user interference channel," *IEEE Trans. Inf. Theory*, vol. 54, no. 8, pp. 3425–3441, Aug. 2008.

[21] T. M. Cover and J. A. Thomas, *Elements of Information Theory*. New York: John Wiley & Sons, Inc., 1991.

[22] R. A. Horn and C. R. Johnson, *Matrix Analysis*. New York: Cambridge University Press, 1990.

[23] M. L. Metha, *Random Matrices*, 3rd ed. London, UK: Academic Press, 2004.

[24] I. S. Gradshteyn and I. M. Ryzhik, *Table of Integrals, Series, and Products*. San Diego: Academic Press, 2000.

APPENDIX A
PROOF OF THEOREM 1

From Lemma 1, we have

$$\mathbb{E}_{\mathbf{H}_l}[\Delta C_l] \approx W \sum_{i=1}^{d_l} \mathbb{E}_{\lambda_i}[\log_2 \lambda_i] \leq W \sum_{i=1}^{d_l} \log_2 \mathbb{E}_{\lambda_i}[\lambda_i].$$

where the last inequality follows from the concavity of the log function and Jensen's inequality. The Marčenko-Pastur theorem [23] says that for a matrix $\mathbf{H}_l$ with $\frac{n_r}{n_t} = \beta$, the limiting p.d.f. of the eigenvalues of the corresponding Wishart matrix $\mathbf{H}_l\mathbf{H}_l^\dagger$ as $n_t, n_r \to \infty$ is:

$$f_\lambda^\beta(x) = \left(1 - \frac{1}{\beta}\right)_+ \delta(x) + \frac{\sqrt{(x-l)_+(u-x)_+}}{2\pi\beta x}, \quad (27)$$

where $l = (1-\sqrt{\beta})^2$, $u = (1+\sqrt{\beta})^2$, and $(\cdot)_+ = \max(0, \cdot)$, and $\delta(x)$ is the Dirac delta function. Moreover, even for small values of n_t and n_r, the p.d.f function in (27) can be used to serve as an excellent approximation [13].

Now, let us first consider the case when $\beta \leq 1$. In this case, the p.d.f. can be simplified to $f_\lambda^\beta(x) = \sqrt{(x-l)_+(u-x)_+}/2\pi\beta x$. Since all eigenvalues are i.i.d. distributed, we have

$$\sum_{i=1}^{d_l} \log_2 \mathbb{E}_{\lambda_i}[\lambda_i] = d_l \log_2 \mathbb{E}[\lambda]$$
$$= d_l \log_2 \left(\frac{1}{2\pi\beta} \int_l^u \sqrt{-x^2 + 2(1+\beta)x - (1-\beta)^2} dx \right).$$

For convenience, let $R(x) = -x^2 + 2(1+\beta)x - (1-\beta)^2$. By using [24, Eq. 2.262], we can derive that

$$\int_l^u \sqrt{R(x)} dx = \frac{2x - 2(1+\beta)}{4} \sqrt{R(x)} \Big|_l^u + \frac{16\beta}{8} \int_l^u \frac{dx}{\sqrt{R(x)}}. \quad (28)$$

Note that the first term in the summation in (28) is zero. Then by using [24, Eq. 2.261], we can further derive that

$$\int_l^u \sqrt{R(x)} dx = 2\beta \arcsin\left(\frac{-2x + 2(1+\beta)}{\sqrt{16\beta}} \right) \Big|_l^u$$
$$= -2\beta(\arcsin(-1) - \arcsin(1)) = 2\pi\beta.$$

It then follows that

$$\mathbb{E}_{\mathbf{H}_l}[\Delta C_l] \leq W \sum_{i=1}^{d_l} \log_2 \mathbb{E}_{\lambda_i}[\lambda_i] = W d_l \log_2 \left(\frac{2\pi\beta}{2\pi\beta} \right) = 0.$$

For the case when $\beta > 1$, the first term in the p.d.f. function in (27) becomes non-zero. Thus, we need to further evaluate the expectation of the first term. In this case, it is easy to see that

$$\int_l^u x \left(1 - \frac{1}{\beta}\right) \delta(x) dx = \left(1 - \frac{1}{\beta}\right) \int_l^u x\delta(x) dx = 0.$$

Combining two cases, we have $\mathbb{E}_{\mathbf{H}_l}[\Delta C_l] \approx 0$ for all β, and the proof is complete.